

The findings in this report are not to be construed as an official Department of the Army position unless so designated by other authorized documents.

Citation of manufacturers' or trade names does not constitute an official endorsement or approval of the use thereof.

Destroy this report when it is no longer needed. Do not return it to the originator.

UNCLASSIFIED

SECURITY CLASSIFICATION OF THIS PAGE

REPORT DOCUMENTATION PAGE				Form Approved OMB No 0704-0188 Exp Date Jun 30, 1986	
1a REPORT SECURITY CLASSIFICATION UNCLASSIFIED		1b. RESTRICTIVE MARKINGS			
2a SECURITY CLASSIFICATION AUTHORITY		3 DISTRIBUTION / AVAILABILITY OF REPORT			
2b DECLASSIFICATION / DOWNGRADING SCHEDULE		Approved for public release; distribution unlimited.			
4 PERFORMING ORGANIZATION REPORT NUMBER(S)		5 MONITORING ORGANIZATION REPORT NUMBER(S) HDL-TR-2138			
6a. NAME OF PERFORMING ORGANIZATION ENSCO, Inc.	6b OFFICE SYMBOL (if applicable)	7a. NAME OF MONITORING ORGANIZATION			
6c. ADDRESS (City, State, and ZIP Code) 5400 Port Royal Road Springfield, VA 22151-2388		7b. ADDRESS (City, State, and ZIP Code)			
8a. NAME OF FUNDING / SPONSORING ORGANIZATION Harry Diamond Laboratories	8b OFFICE SYMBOL (if applicable) SLCHD-NW-ED	9. PROCUREMENT INSTRUMENT IDENTIFICATION NUMBER			
8c. ADDRESS (City, State, and ZIP Code) 2800 Powder Mill Road Adelphi, MD 20783-1197		10. SOURCE OF FUNDING NUMBERS			
		PROGRAM ELEMENT NO. 6.21.20.A	PROJECT NO.	TASK NO.	WORK UNIT ACCESSION NO.
11. TITLE (Include Security Classification) Validity of Equivalent Source Representation for Coaxially Shielded Cables and Multiconductor Cables					
12 PERSONAL AUTHOR(S) Robert F. Gray					
13a TYPE OF REPORT Technical Report	13b TIME COVERED FROM Jan 86 TO Sep 87	14 DATE OF REPORT (Year, Month, Day) March 1988	15 PAGE COUNT 35		
16. SUPPLEMENTARY NOTATION AMS code: 612120.H250011; HDL project: XE75E4					
17 COSATI CODES		18. SUBJECT TERMS (Continue on reverse if necessary and identify by block number)			
FIELD	GROUP	SUB-GROUP	Electromagnetic pulse, cable terminations, direct injection, coaxial cables, shield multiconductor cables, transfer impedance, propagation constant,		
19 ABSTRACT (Continue on reverse if necessary and identify by block number)					
Efficient equivalent source representations were developed for coaxially shielded cables and for multiconductor cables. The correctness of these equivalent source representations was validated by linear and nonlinear terminations. The distribution of shield coupling parameters was studied for shielded multiconductor cables. The results of this study indicated that an approximate equivalent source excitation may be used for multiconductor cables, thereby reducing the source requirements even further. The approximate equivalent source excitation requires only two independent sources to represent the EMP response of the cable. The simplicity of the equivalent source excitation means that numerical models will run quicker, and system-level stimulation is possible with a lower power level and less complex simulators.					
20 DISTRIBUTION / AVAILABILITY OF ABSTRACT <input checked="" type="checkbox"/> UNCLASSIFIED/UNLIMITED <input type="checkbox"/> SAME AS RPT <input type="checkbox"/> DTIC USERS		21 ABSTRACT SECURITY CLASSIFICATION UNCLASSIFIED			
22a NAME OF RESPONSIBLE INDIVIDUAL John Beilfuss		22b TELEPHONE (Include Area Code) (703) 490-2411/2404		22c OFFICE SYMBOL SLCHD-NW-ED	

DD FORM 1473, 84 MAR

83 APR edition may be used until exhausted  
All other editions are obsolete

SECURITY CLASSIFICATION OF THIS PAGE

UNCLASSIFIED

UNCLASSIFIED

SECURITY CLASSIFICATION OF THIS PAGE

18. SUBJECT TERMS (cont'd)

equivalent sources, voltage substitution, non-linear loads, transmission-line, Thevenin's & Norton's Theorems, piecewise-linear

Accession For	
NTIS CRA&I	<input checked="" type="checkbox"/>
DTIC TAB	<input type="checkbox"/>
Unannounced	<input type="checkbox"/>
Justification:	
By	
Distribution/	
Availability Codes	
Dist	Avail and/or Special
A-1	



UNCLASSIFIED

SECURITY CLASSIFICATION OF THIS PAGE

## CONTENTS

	<u>Page</u>
1. INTRODUCTION.....	5
2. RESPONSE OF A COAXIALLY SHIELDED CABLE.....	5
2.1 Distributed Excitation.....	5
2.2 Equivalent Excitation.....	7
2.2.1 Thevenin's and Norton's Theorems.....	7
2.2.2 Thevenin Equivalent Representation.....	8
2.2.3 Nonlinear Terminations.....	10
3. RESPONSE OF A MULTICONDUCTOR TRANSMISSION LINE.....	16
3.1 Distributed Excitation.....	16
3.2 Equivalent Excitation.....	20
3.2.1 Thevenin Source Terms.....	20
3.2.2 Terminal Response.....	22
3.2.3 Nonlinear Terminations.....	23
3.2.4 Coupling Distribution.....	23
3.3 Equivalent Excitation Implementation.....	27
4. CONCLUSION .....	30
REFERENCES .....	30
DISTRIBUTION .....	31

## FIGURES

1. Transmission line with distributed excitation.....	6
2. Interconnected networks.....	7
3. Equivalent network for coaxial cable.....	10
4. Piecewise-linear representation of nonlinear load.....	11
5. Piecewise-linear solution.....	12
6. Terminal response of coaxial cable.....	14
7. Open circuit voltages after time $t_0$ .....	14

FIGURES (cont'd)

	<u>Page</u>
8. Multiconductor transmission line.....	17
9. Generalized point source for multiconductor transmission line...	18
10. Equivalent source representation for multiconductor transmission line.....	21
11. Multiconductor transmission-line segment.....	25
12. Equivalent source implementation using resistors in shield.....	29
13. Equivalent source implementation over entire cable shield.....	29

## 1. INTRODUCTION

The electromagnetic pulse (EMP) analysis of a system frequently focuses on the response of cables excited by the transient fields. A large variety of analysis tools and techniques is available to aid in the study of the cable response. EMP simulators are available for experimental studies of system response. Difficulties arise, however, when we attempt to incorporate the results of cable coupling codes into circuit analysis codes for damage assessments. Similarly, obtaining threat-level responses with typical simulators is possible for only very short cables and compact systems. This report presents a solution to these problems using an equivalent source representation of the cable. Initially, the technique is developed for a single coaxially shielded cable. Then the approach is extended to multiconductor cables.

## 2. RESPONSE OF A COAXIALLY SHIELDED CABLE

The response of a coaxial cable due to a distributed excitation is reviewed in section 2.1. An equivalent and more compact source representation is developed in section 2.2. Section 2.3 investigates the validity of the equivalent representation when the line is loaded with nonlinear terminations.

### 2.1 Distributed Excitation

The response of a coaxially shielded cable with distributed excitation may be treated like the two-wire line problem shown in figure 1. The distributed voltage source,  $V_s(x, \omega)$ , is related to the complex transfer impedance of the shield and the external current flowing on it. The distributed current source,  $I_s(x, \omega)$ , accounts for coupling through the holes of the shield. Detailed explanations of the shield coupling mechanisms and solutions of the coupling problem are provided in numerous reports (e.g., [1], [2], [3]).\* For this paper it is sufficient to define the general coupling problem as two arbitrary distributed sources--a series voltage source and a shunt current source. The transmission line of figure 1 has a characteristic impedance,  $K$ , a propagation characteristic,  $\Gamma$ , and linear terminations  $Z_1$  and  $Z_2$  at  $x = 0, l$ , respectively.

Schelkunoff [4] provides a solution for the terminal response of the transmission line shown in figure 1:

$$\begin{aligned} V(0) &= \int_0^l V_s(\xi) G_{V_1}(0, \xi) d\xi + \int_0^l I_s(\xi) G_{V_2}(0, \xi) d\xi \\ &= -\frac{KZ_1}{D} \int_0^l V_s(\xi) \{K \cosh \Gamma(l - \xi) + Z_2 \sinh \Gamma(l - \xi)\} d\xi - \end{aligned}$$

\*References are listed at end of report.

$$\begin{aligned}
& - \frac{K^2 Z_1}{D} \int_0^1 I_s(\xi) \{K \sinh \Gamma(1-\xi) + Z_2 \cosh \Gamma(1-\xi)\} d\xi \\
V(1) &= \int_0^1 V_s(\xi) G_{V_1}(1, \xi) d\xi + \int_0^1 I_s(\xi) G_{V_2}(1, \xi) d\xi \\
&= \frac{K Z_2}{D} \int_0^1 V(\xi) \{K \cosh \Gamma \xi + Z_1 \sinh \Gamma \xi\} d\xi \\
& - \frac{K^2 Z_1}{D} \int_0^1 I_s(\xi) \{K \sinh \Gamma \xi + Z_1 \cosh \Gamma \xi\} d\xi
\end{aligned}$$

where

$$D = K \left[ (K^2 + Z_1 Z_2) \sinh \Gamma + K(Z_1 + Z_2) \cosh \Gamma \right] \quad (1)$$

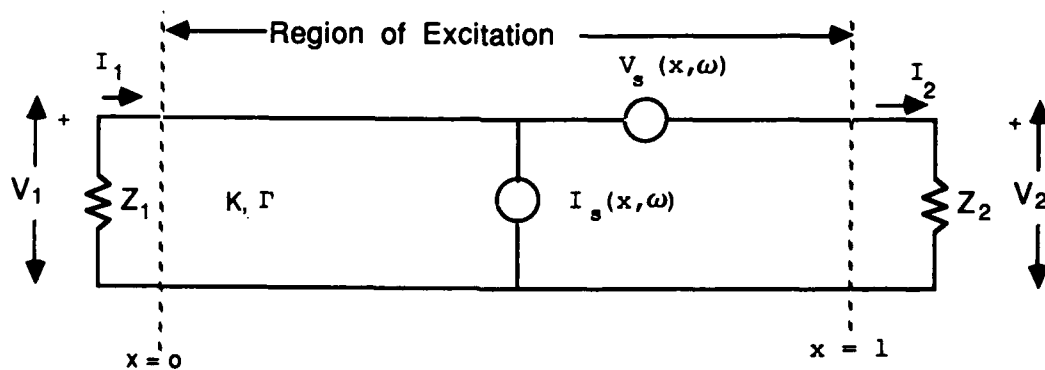


Figure 1. Transmission line with distributed excitation.

The line response may be computed using the proper frequency descriptions of the line parameters, terminations, and source functions. The time domain response is then obtained using a suitable inverse Fourier transform.

## 2.2 Equivalent Excitation

It is desired to develop an equivalent model of the transmission line problem of figure 1. Characteristics of the model should include a simplified source characterization, ease of implementation in circuit analysis codes, applicability to nonlinear loading, and a relatively easy physical implementation for testing purposes. Equivalent source theory will be reviewed briefly before an alternate coaxial cable coupling model is developed.

### 2.2.1 Thevenin's and Norton's Theorems

Both Thevenin's and Norton's theorems deal with the development of equivalent source representations of a linear network,  $N$ , that excites an arbitrary load network,  $N'$ , as shown in figure 2. Thevenin's theorem states that the network  $N$  may be replaced by an equivalent generator consisting of a voltage source and a series internal impedance such that the terminal response (current and voltage at  $T_1, T_2$ ) will be identical to the original network ( $N$  and  $N'$ ). An equivalent current source representation may be developed through the application of Norton's theorem.

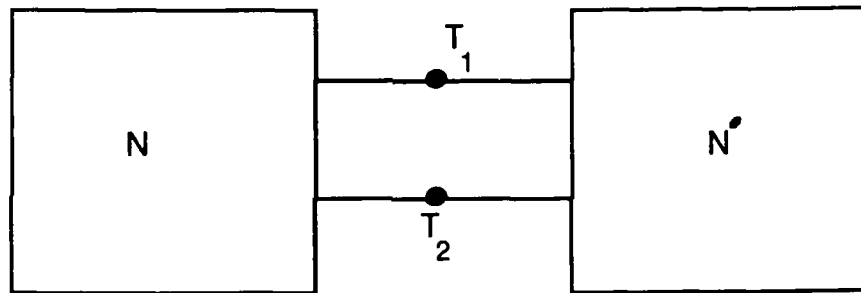


Figure 2. Interconnected networks.

Peskin [5] develops Thevenin's and Norton's theorems subject to the following assumptions:

- (a) The network  $N$  in figure 2 is linear.
- (b) The network  $N$  is stable over the full range of load values possible.
- (c) The terminal response is Laplace transformable; this does not require  $N'$  to be linear; only its load voltage and current must obey

$$\int_0^{\infty} |f(t)| e^{-\sigma t} dt < \infty ,$$

for some real number,  $\sigma$ .

Using these assumptions and the node relationships, it is a relatively straightforward matter to prove that the network N may be replaced by a voltage source equal to the open circuit voltage at terminals T1,T2 and a series impedance equal to the input impedance of N looking into T1,T2. The input impedance is found by shorting out all independent voltage sources and opening all independent current sources. The Norton equivalent uses a current generator equal to the short circuit current at T1,T2 shunted by the input admittance (the reciprocal of the input impedance).

This two-terminal or single port theorem can be extended to multiport networks if we require m independent sources, one for each of m ports, and if we define an impedance (admittance) matrix composed of the self impedance (admittance) and transfer impedance (admittance) from each of the other ports. The source voltages for a Thevenin equivalent network are defined by

$$V_k^{oc} = V_k, \quad I_j = 0, \quad j=1, m, \quad (2)$$

where  $V_k$  is the potential at port k and  $I_j$  is the current through port j. Similarly, the Norton current sources are the short circuit currents at each port when all the ports are shorted. The impedance matrix for the Thevenin representation is defined by the equation

$$z_{ij} = V_i/I_j, \quad I_k = 0, \quad \forall K \neq j, \quad (3)$$

under the condition that all internal independent sources are properly shut off. The admittance matrix is the inverse of the impedance matrix. The multiport Thevenin theorem will be applied in the next section to develop an equivalent representation of the coaxially shielded cable.

### 2.2.2 Thevenin Equivalent Representation

Modeling the coaxial cable response with a Thevenin equivalent generator requires computation of the open circuit voltage at each end. Using equation (1) and letting  $Z_1, Z_2$  approach infinity yields the following open circuit voltages:

$$V_{oc}(0) = - \int_0^1 V_s(\xi) \frac{\sinh \Gamma(1-\xi)}{\sinh \Gamma} d\xi - K \int_0^1 I_s(\xi) \frac{\cosh \Gamma(1-\xi)}{\sinh \Gamma} d\xi$$

and

$$V_{oc}(1) = \int_0^1 V_s(\xi) \frac{\sinh \Gamma \xi}{\sinh \Gamma} d\xi - K \int_0^1 I_s(\xi) \frac{\cosh \Gamma \xi}{\sinh \Gamma} d\xi. \quad (4)$$

Figure 3 shows the equivalent network. The impedance matrix,  $Z$ , is simply

$$\bar{Z} = \begin{bmatrix} K/\tanh \Gamma & -K/\sinh \Gamma \\ K/\sinh \Gamma & -K/\tanh \Gamma \end{bmatrix}, \quad (5)$$

and the terminal response is given by

$$\bar{V} = \begin{bmatrix} V_1 \\ V_2 \end{bmatrix} = \bar{Z} \begin{bmatrix} I_1 \\ I_2 \end{bmatrix} + \begin{bmatrix} V_s^1 \\ V_s^2 \end{bmatrix} = \bar{Z}\bar{I} + \bar{V}_s. \quad (6)$$

Using the impedance relationship for the load voltage and current,  $I_1 = -V_1/Z_1$  and  $I_2 = V_2/Z_2$ , the load voltage is found from equation (6):

$$\bar{V} = \bar{Z} \begin{bmatrix} -1/z_1 & 0 \\ 0 & 1/z_2 \end{bmatrix} \bar{V} + \bar{V}_s. \quad (7)$$

Equation (7) may be solved for  $V$  as follows:

$$\begin{aligned} V &= \left[ \bar{u} - \bar{Z} \begin{bmatrix} -1/z_1 & 0 \\ 0 & 1/z_2 \end{bmatrix} \right]^{-1} \bar{V}_s \\ &= \begin{bmatrix} 1 + K/(z_1 \tanh \Gamma) & K/(z_2 \sinh \Gamma) \\ K/(z_1 \sinh \Gamma) & 1 + K/(z_2 \tanh \Gamma) \end{bmatrix}^{-1} \bar{V}_s \\ &= \frac{K}{D} \begin{bmatrix} z_1 [z_2 \sinh \Gamma + K \cosh \Gamma] & -z_1 \\ -z_2 & z_2 [z_1 \sinh \Gamma + K \cosh \Gamma] \end{bmatrix} \bar{V}_s, \quad (8) \end{aligned}$$

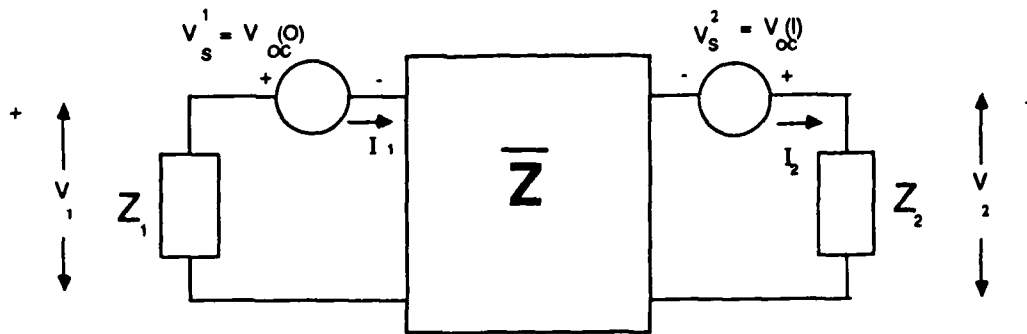


Figure 3. Equivalent network for coaxial cable.

where  $\bar{u}$  is the identity matrix. After substitution of equation (4) for the source term,  $\bar{V}_s$ , manipulation of equation (8) yields equation (1), demonstrating the correctness of the equivalent network.

The advantages of the equivalent representation are that the distributed source is replaced by two point sources and the excitation is separated from the transmission line. This means that standard transmission-line models available in most circuit analysis codes may be used in conjunction with two voltage sources to model the coaxial cable. Similarly, from a simulation standpoint, an injection system may be developed using two independent voltage sources, one for each end of the cable. Therefore, the objective of developing a simplified representation for the EMP coupling to a coaxial cable has been achieved. The one area not fully explored is the correctness of the equivalent representation when nonlinear loads appear at the terminals in place of  $Z_1$  and  $Z_2$ . Nonlinear loading is studied in the next section.

### 2.2.3 Nonlinear Terminations

It was demonstrated that the equivalent Thevenin representation for the coaxial cable produced results identical to the distributed excitation when linear terminations are used. While the single port representation is valid for nonlinear loads, nothing has been done to validate the multi-port representation of distributed networks with nonlinear loads. In the following analysis it is assumed that the transmission line is linear and that the potentials created because of the EMP excitation do not exceed the dielectric breakdown voltages for the cable. Note that this does not preclude the inclusion of nonlinear effects on the exterior of the cable; only its internal line must be linear. If internal breakdown is possible, then the model would have to be further partitioned to isolate the nonlinear regions.

Obtaining a closed form solution for the response of a transmission line with nonlinear loads is in all probability impossible. However, if a slight restriction is placed on the nature of the terminations, the problem becomes fairly straightforward, and useful insight may be gained into the actual line response. As illustrated in figure 4, it is possible to very closely approximate a nonlinear load characteristic with a set of linear curves. The piecewise-linear approach will be used to study the validity of the equivalent transmission line representation under nonlinear loading.

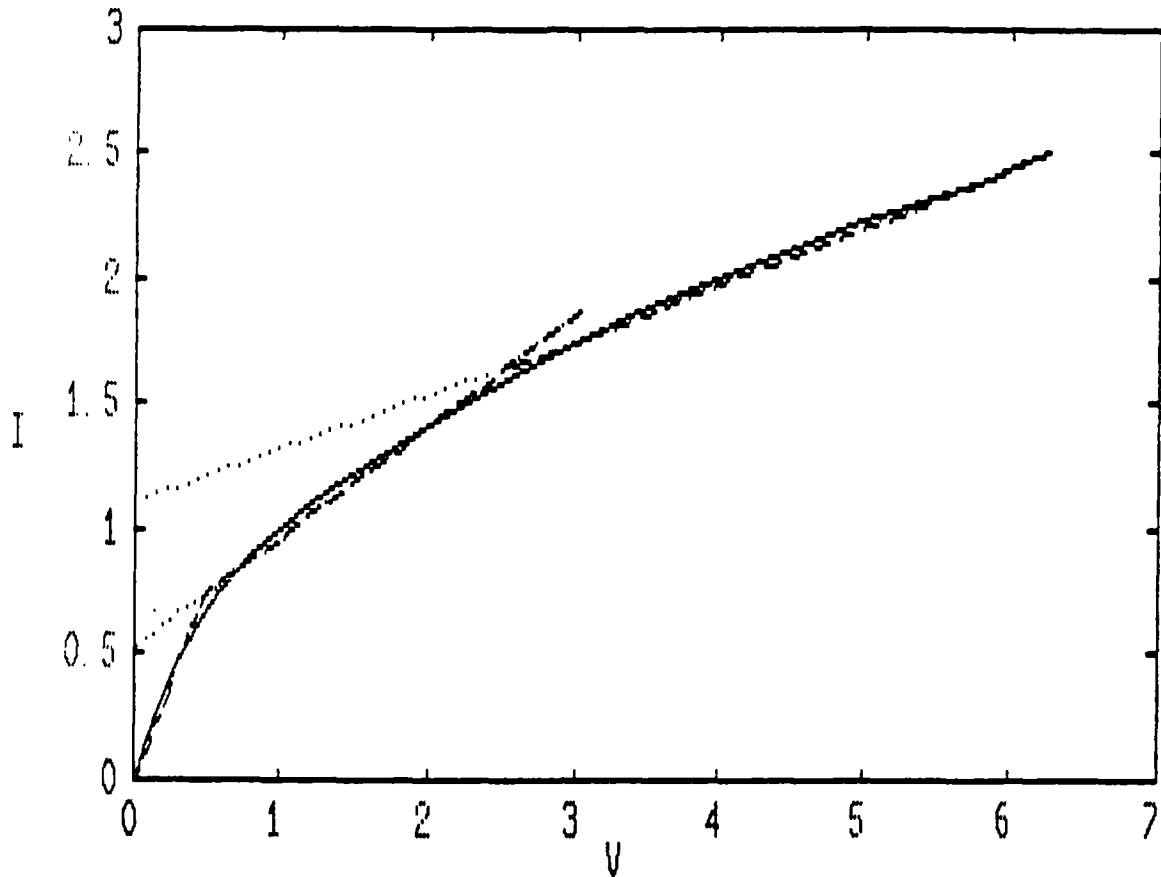


Figure 4. Piecewise-linear representation of nonlinear load.

Solving for the response with nonlinear loads simply involves a series of linear solutions, with the loading over a specific time period being determined by the load voltage or current. The only complication in the solution is the inclusion of initial condition effects at transition points.

An example of how a piecewise-linear solution is used is presented in figure 5. Here the response of a circuit loaded by the simple square law device of figure 4 is computed. As the load current,  $I$ , reaches a transition value of the piecewise-linear model, a new linear equation must be solved. In practice, only a finite number of segments will be used to represent the nonlinear load. However, if computation load is not a consideration, then a very large set of linear curves may be used to achieve any desired accuracy. The current response shown in figure 5 was calculated with only two linear regions. The piecewise-linear response compared within one percent with the response computed with the MICROCAP-II circuit analysis code.

The solution for the EMP response of the coaxial cable given in equation (1) assumed that the initial conditions were zero. The effect of the nonzero initial conditions at different points in time is seen in the transforms of the differential equations describing the transmission line

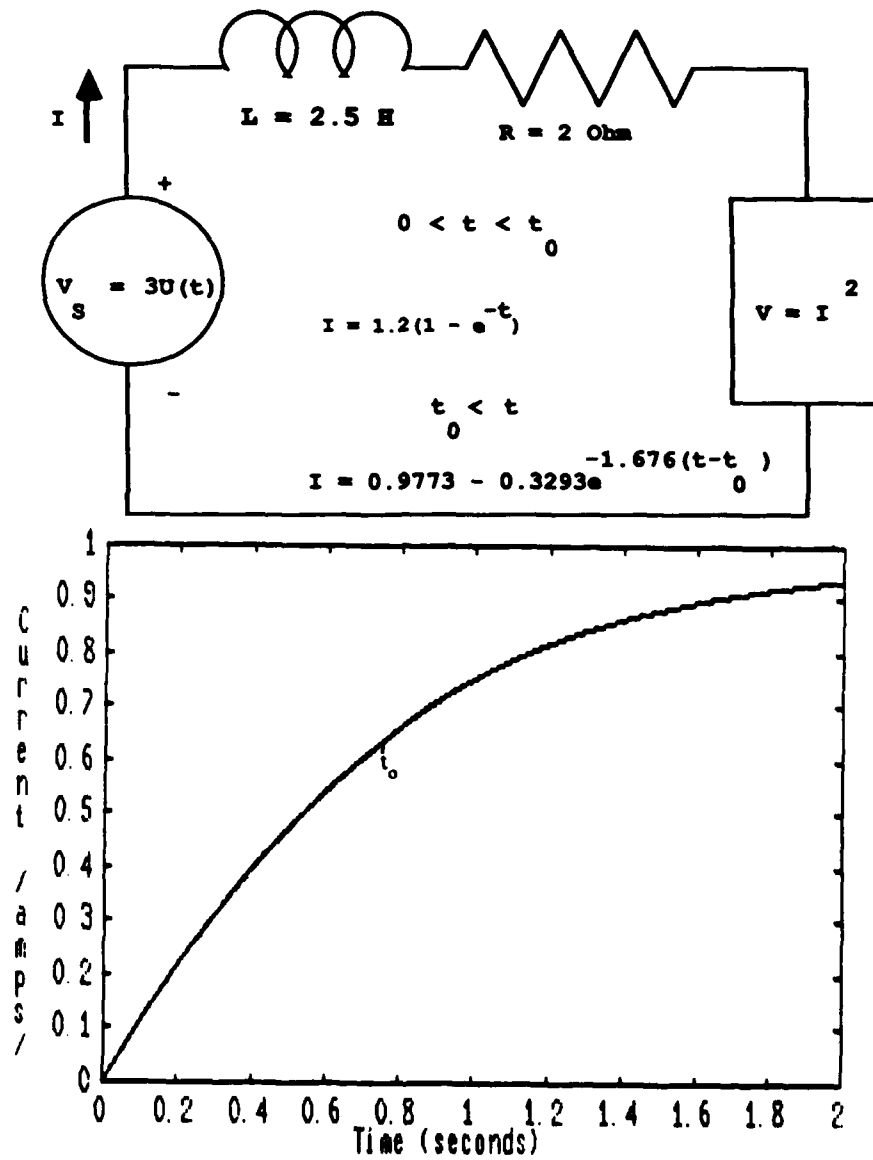


Figure 5. Piecewise-linear solution.

$$\frac{dV}{dx} = -(R + j\omega L)I + LI(t_0) + V_s$$

$$\frac{dI}{dx} = -(G + j\omega C)V + CV(t_0) + I_s \quad (9)$$

The effect of the initial conditions is to add constant source terms,  $LI(t_0)$  and  $CV(t_0)$ , to the EMP sources,  $V_s$  and  $I_s$ . Defining two new source terms,

$$V'_s = V_s + L I(t_0)$$

and

$$I'_s = I_s + C V(t_0); \quad (10)$$

the transmission-line response is given by equation (1) with the new source terms. Therefore, from a computational standpoint, a new Thevenin equivalent generator is needed to model the line after a transition has occurred in one of the terminations. The impedance matrix,  $Z$ , remains unchanged, but the sources at each end are now

$$\begin{aligned} V_{oc}(0) &= - \int_0^l V'_s(\xi) \frac{\sinh \Gamma(1-\xi)}{\sinh \Gamma} d\xi - K \int_0^l I'_s(\xi) \frac{\cosh \Gamma(1-\xi)}{\sinh \Gamma} d\xi \\ V_{oc}(l) &= \int_0^l V'_s(\xi) \frac{\sinh \Gamma \xi}{\sinh \Gamma} d\xi - K \int_0^l I'_s(\xi) \frac{\cosh \Gamma \xi}{\sinh \Gamma} d\xi \end{aligned} \quad (11)$$

Therefore, the criterion for determining the validity of the Thevenin equivalent network with nonlinear loading is whether or not it produces the open circuit voltages defined in equation (11) after load transitions. The question arises not because of the distributed EMP sources,  $V_s$  and  $I_s$ , but rather because of the initial conditions,  $I(t_0)$  and  $V(t_0)$ . Obviously, the transmission-line current and voltage distributions are different for the actual EMP excitation and its Thevenin equivalent. If the proper open circuit voltage is produced after time  $t_0$ , then the Thevenin equivalent network is valid even when nonlinear loads are used.

One method of verifying the correctness of the open circuit voltages would be to (1) compute the complete line response under both types of excitation, (2) transform the response into the time domain to obtain the initial condition distribution along the line, and (3) solve for the open circuit voltages with the distributed initial conditions,  $V(t_0)$  and  $I(t_0)$ , and EMP source terms,  $V_s$  and  $I_s$ . Unfortunately, it is very difficult to verify open circuit voltages, even for a simple circuit. A similar approach was used to analyze a two-section lumped parameter transmission-line model [6]. Based on the complexity encountered with only a simple circuit, it is not likely that a general solution can be obtained. Therefore, a different approach is needed.

Assume that the terminal responses of a coaxial cable are as shown in figure 6. Let there be a nonlinearity in the termination at  $x = 0$  such that the impedance,  $Z_1$ , changes due to the voltage at time  $t_0$ . Next, assume that the open circuit voltages from time  $t_0$  on are as shown in figure 7. Note that these open circuit voltages are different from the voltages starting at time  $t_0$  due to the loading from time zero to  $t_0$ . These open circuit voltages may now be used to compute the response of the line after the nonlinear transition at time  $t_0$  as shown in figure 6 by the dashed waveforms.

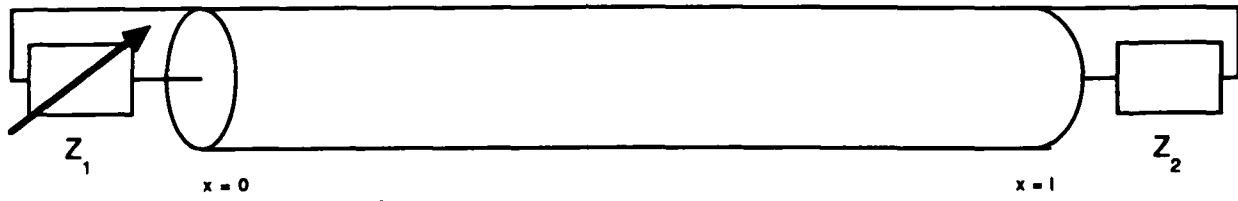
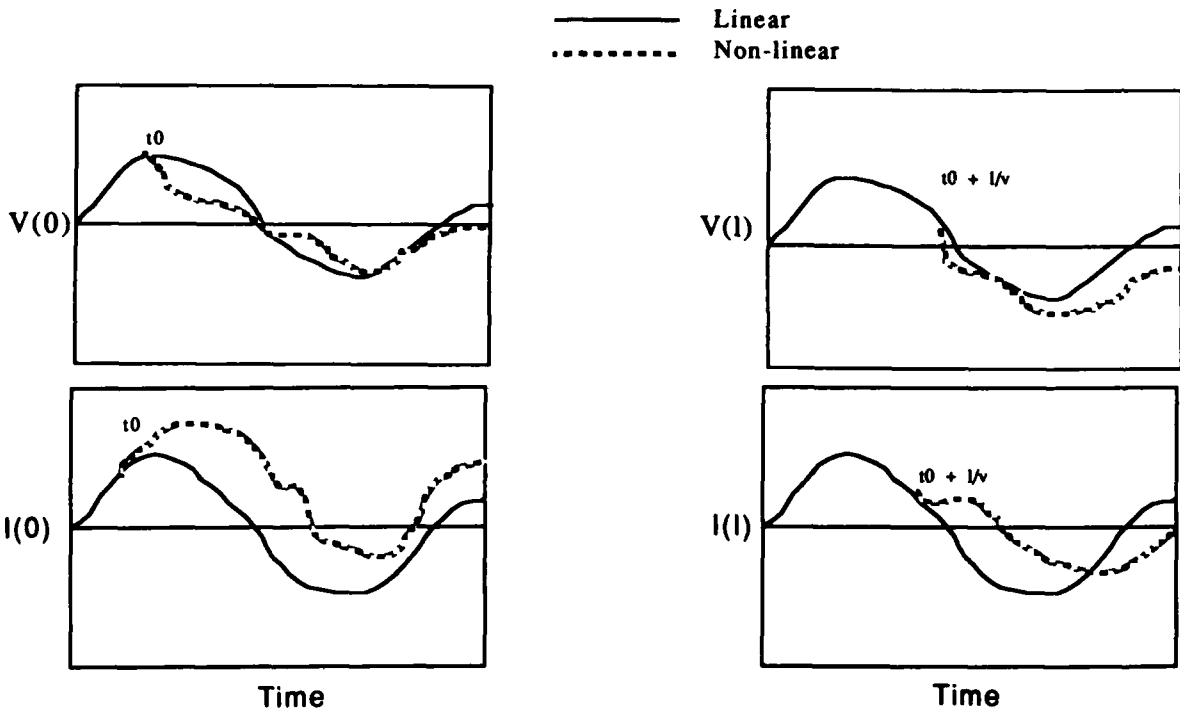


Figure 6. Terminal response of coaxial cable.

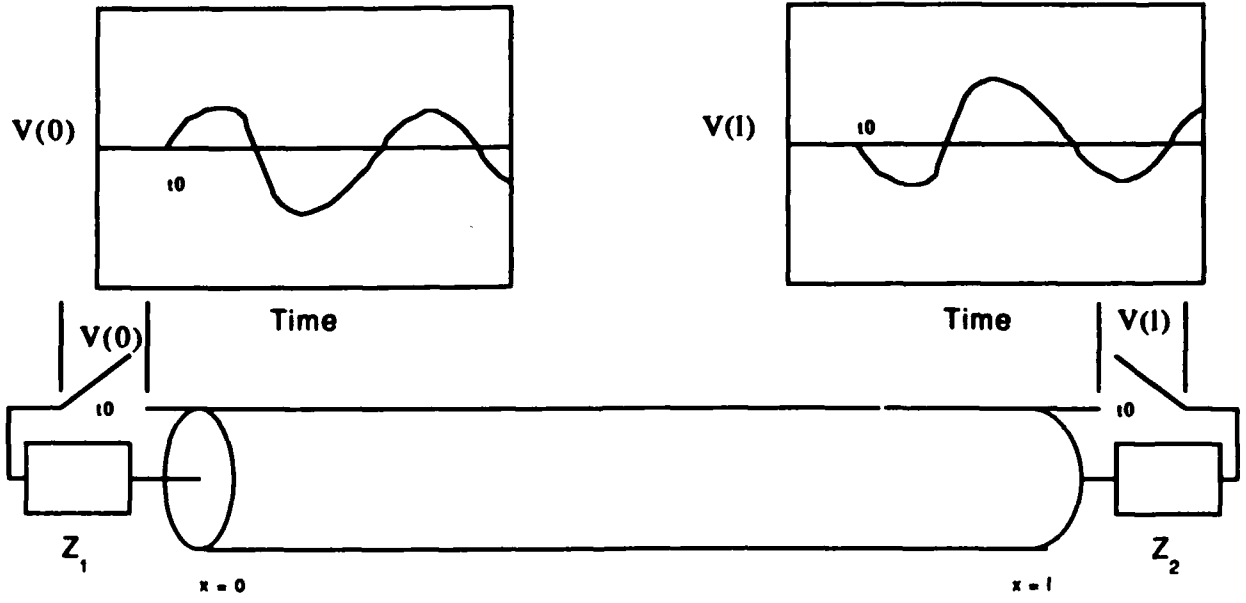


Figure 7. Open circuit voltages after time  $t_0$ .

Using contradiction, we will now prove the validity of using a Thevenin equivalent network to model the response of a transmission line with nonlinear loading. In section 2.2.2 it was shown that the response of the Thevenin network would duplicate the line response with linear loads (the solid curves in fig. 6). Now assume that the open circuit voltages of the equivalent circuit after time  $t_0$  are not the same as figure 7. This is the only way the equivalent network will not provide the correct response after the transition at time  $t_0$ . We now have two different networks for times greater than  $t_0$ , one with the correct open circuit voltages from the actual transmission line and one with incorrect open circuit voltages from the original Thevenin equivalent network. The impedance networks are identical because of the assumption that the line is linear and operating below breakdown. In section 2.2.2 it was shown that a Thevenin equivalent network will provide correct terminal responses for any linear loading. Now reconnect the original terminations,  $Z_1$  and  $Z_2$ , to the new equivalent network. Since it was assumed that the open circuit voltages from the original Thevenin model are incorrect, the response with the original loading is also incorrect. This violates the work of section 2.2.2 that proved that the Thevenin equivalent would provide the proper response for all time with a linear load. Therefore, the assumption must be false that the open circuit voltages produced by the equivalent network are different from the open circuit voltages produced by the actual distributed excitation.

An alternate approach for validating the Thevenin equivalent network can be developed that uses the uniqueness of the solution for the transmission line differential equations.

Since the differential equations governing the transmission line are linear and time invariant, the solution for a given input and initial state is unique. This implies that the input required to produce a specified output from an initial condition set is also unique.

The open circuit voltages,  $V_s'$ , required to produce a given terminal response,  $V_1(t_0)$  and  $V_2(t_0)$ , starting from time,  $t_0$ , are found from equation (8) to be

$$\bar{V}_s' = \begin{bmatrix} V_s^1(t_0) \\ V_s^2(t_0) \end{bmatrix} = \left[ \bar{u} - \bar{Z} \begin{bmatrix} -1/z_1 & 0 \\ 0 & 1/z_2 \end{bmatrix} \right] \begin{bmatrix} V_1(t_0) \\ V_2(t_0) \end{bmatrix}, \quad (12)$$

where the voltages  $V_1(t_0)$  are the Fourier transforms of the time domain waveforms from time  $t_0$  on. Since the actual network response and its Thevenin equivalent produce identical terminal responses with linear loads,  $Z_1$  and  $Z_2$ , the open circuit voltages from time  $t_0$  must be identical. Otherwise, more than one set of inputs will provide the same outputs. This is not possible with a linear line. The effective open circuit voltages starting at an arbitrary time  $t_0$  due to the impressed sources and the initial conditions must be the same for the actual line with distributed excitation and its Thevenin counterpart with only two source terms. Therefore, both lines will provide the same terminal response after a termination transition at a time,  $t_0$ .

Equation (12) suggests a method for solving for the response of a coaxial line with nonlinear terminations using Fourier transform techniques. The load nonlinearity is assumed to be piecewise-linear. The steps to solve for the nonlinear response are as follows:

- (a) Compute the complete terminal response with the nominal values for the terminations. This is done in the frequency domain and transformed into the time domain.
- (b) Determine the time,  $t_0$ , where a transition will occur in a termination.
- (c) Compute the effective open circuit voltage with a start time of  $t_0$ . These voltages are found by computing the Fourier transforms of the terminal responses multiplied by a unit step function starting at  $t_0$ . Alternatively this may be accomplished by convolution of the frequency response at the terminals with a unit step defined by

$$\bar{V}'_s = \left[ \bar{u} - \bar{z} \begin{bmatrix} -1/z_1 & 0 \\ 0 & 1/z_2 \end{bmatrix} \right] \left[ \bar{f} \left\{ u(t-t_0) * \begin{bmatrix} V_1 \\ V_2 \end{bmatrix} \right\} \right] \quad (13)$$

- (d) Solve for the terminal response after the transition ( $t \geq t_0$ ) using equation (8), the source voltages from step 3, and the new terminations.

This is a simple approach to solving a complex problem. This technique should be computationally superior to finite difference techniques when the line lengths are long and many cells would be needed to model the transmission line.

### 3. RESPONSE OF A MULTICONDUCTOR TRANSMISSION LINE

The equivalent source representation developed in section 2 for simple coaxial cables will now be extended to multiconductor transmission lines. After a brief review of multiconductor transmission line theory in section 3.1, the equivalent source representation is developed in section 3.2. Several implementation techniques are reviewed in section 3.3.

#### 3.1 Distributed Excitation

Consider the lossless multiconductor transmission line shown in figure 8. The line consists of  $N + 1$  conductors, with conductor  $N + 1$  being the reference conductor. The length of the line is  $l$ , and its electrical

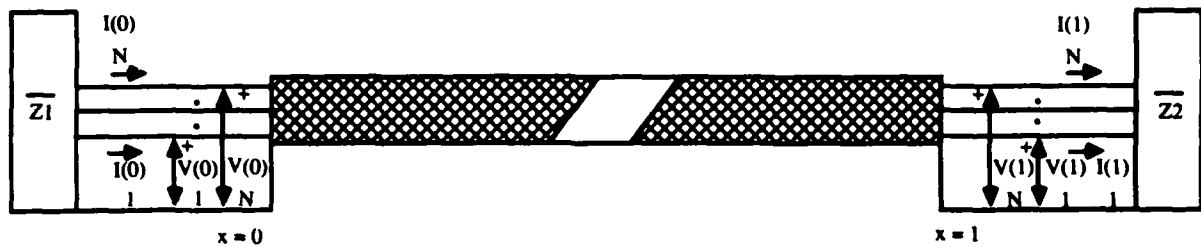


Figure 8. Multiconductor transmission line.

characteristics are determined by the capacitive coefficient matrix  $C$  and the inductive coefficient matrix  $L$ . The line is described by the following matrix partial differential equations [7]:

$$\frac{\partial \bar{v}(x,t)}{\partial x} = -\bar{L} \frac{\partial \bar{i}(x,t)}{\partial t}$$

$$\frac{\partial \bar{i}(x,t)}{\partial x} = -\bar{C} \frac{\partial \bar{v}(x,t)}{\partial t} \quad (14)$$

when no source terms are present. Using the Laplace transform these equations become:

$$\frac{\partial}{\partial x} \begin{bmatrix} \bar{V} \\ \bar{I} \end{bmatrix} = -s \begin{bmatrix} \bar{0} & \bar{L} \\ \bar{C} & \bar{0} \end{bmatrix} \begin{bmatrix} \bar{V} \\ \bar{I} \end{bmatrix}, \quad (15)$$

where the dependence of  $\bar{V}$  and  $\bar{I}$  on  $x$  is implicit;  $\bar{V}$  and  $\bar{I}$  are  $n \times 1$  vectors;  $\bar{L}$  and  $\bar{C}$  are  $n \times n$  matrices and  $\bar{0}$  is a zero matrix of order  $n \times n$ .

Differentiating equation (14) and substituting yield a set of decoupled second-order differential equations:

$$\frac{\partial^2}{\partial x^2} \begin{bmatrix} \bar{V} \\ \bar{I} \end{bmatrix} = +s^2 \begin{bmatrix} \bar{L}\bar{C} & \bar{0} \\ \bar{0} & \bar{C}\bar{L} \end{bmatrix} \begin{bmatrix} \bar{V} \\ \bar{I} \end{bmatrix}. \quad (16)$$

It is possible for lossless multiconductor cables to define a transformation matrix  $T$  such that

$$s^2 \bar{T}^{-1} \bar{C}\bar{L}\bar{T} = \bar{\gamma}^2, \quad (17)$$

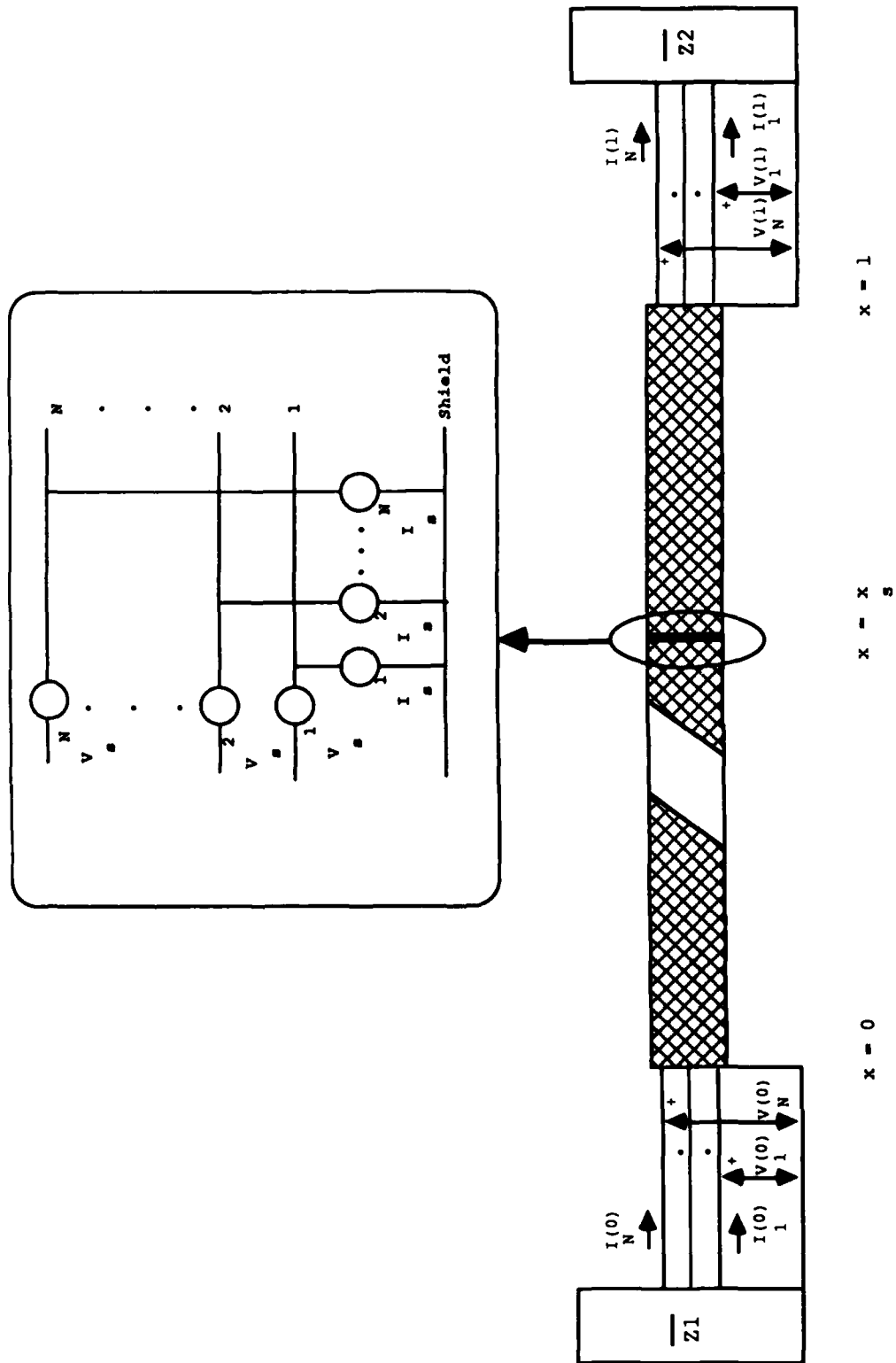


Figure 9. Generalized point source for multiconductor transmission line.

where  $\bar{\gamma}$  is an  $n \times n$  diagonal matrix with elements

$$\gamma_{ij}^2 = \begin{cases} \gamma_i^2, & i = j \\ 0, & i \neq j \end{cases}, \quad (18)$$

and  $\gamma_1$  an eigenvalue of equation (16).

Then using the transformations  $\bar{V} = \bar{T}\bar{V}'$  and  $\bar{I} = \bar{T}\bar{I}'$ , equation (16) becomes a set of  $2N$  decoupled differential equations with a solution given by

$$\begin{bmatrix} \bar{V} \\ \bar{I} \end{bmatrix} = \begin{bmatrix} \bar{Z}_c & -\bar{Z}_c \\ \bar{U} & \bar{U} \end{bmatrix} : \begin{bmatrix} \bar{T}e^{-\bar{\gamma}x} \bar{\alpha}^+ \\ \bar{T}e^{\bar{\gamma}x} \bar{\alpha}^- \end{bmatrix}, \quad (19)$$

where

$$\bar{Z}_c = s^{-1} \bar{C}^{-1} \bar{T} \bar{\gamma} \bar{T}^{-1} \quad (20)$$

is the characteristic impedance matrix,  $\bar{U}$  is the identity matrix, and  $\bar{\alpha}^+$  and  $\bar{\alpha}^-$  are  $n \times 1$  vectors determined by the terminating impedances and the source terms exciting the line. Tesche et al [7] provide a solution for  $\bar{\alpha}^+$  and  $\bar{\alpha}^-$  when the line is terminated in impedance matrices  $Z_1, Z_2$  at  $x = 0$  and  $x = 1$ , respectively, and in a generalized point source at  $x_s$ , as shown in figure 9. Of interest here is the terminal response of the line. The voltage and current at the ends are related by the terminating matrices as follows:

$$\begin{bmatrix} \bar{V}(0) \\ \bar{V}(1) \end{bmatrix} = \begin{bmatrix} -\bar{Z}_1 & \bar{0} \\ \bar{0} & \bar{Z}_2 \end{bmatrix} : \begin{bmatrix} \bar{I}(0) \\ \bar{I}(1) \end{bmatrix}, \quad (21)$$

and from Frankel [8],

$$\begin{bmatrix} \bar{I}(0) \\ \bar{I}(1) \end{bmatrix} = \begin{bmatrix} \bar{U} - \bar{\Gamma}_1 & \bar{0} \\ \bar{0} & \bar{U} - \bar{\Gamma}_2 \end{bmatrix} : \begin{bmatrix} \bar{\Gamma}_1^{-1} & \bar{T}e^{\bar{\gamma}} \bar{T}^{-1} \\ \bar{T}e^{\bar{\gamma}} \bar{T}^{-1} & \bar{\Gamma}_2^{-1} \end{bmatrix} : \begin{bmatrix} \bar{\delta}^- \\ \bar{\delta}^+ \end{bmatrix}, \quad (22)$$

where

$$\bar{\Gamma}_i = [\bar{Z}_i + \bar{Z}_c]^{-1} [\bar{Z}_i - \bar{Z}_c] \quad (23)$$

is the reflection coefficient associated with load impedance  $Z_i$ , and  $\bar{\delta}^-$  and  $\bar{\delta}^+$  are source-related terms. The operator ":" in the above equations arises from the fact that the elements of the matrices are also matrices. The matrices are first multiplied as if they contained normal scalar elements. Then the resulting matrix operations for each element are carried out.

The source terms  $\bar{\delta}^-$  and  $\bar{\delta}^+$  have been presented [9] for a generalized point source (fig. 9) as

$$\begin{bmatrix} \bar{\delta}^- \\ \bar{\delta}^+ \end{bmatrix} = 1/2 \begin{bmatrix} \bar{T} e^{-\gamma x_s} \bar{T}^{-1} \\ \bar{T} e^{\gamma x_s} \bar{T}^{-1} \end{bmatrix} : \begin{bmatrix} \bar{Z}_c^{-1} & \bar{U} \\ \bar{Z}_c^{-1} & -\bar{U} \end{bmatrix} : \begin{bmatrix} \bar{V}_s \\ \bar{I}_s \end{bmatrix}, \quad (24)$$

where  $x_s$  is the location of the source. If a distributed source excites the line then equation (22) must be integrated over the source:

$$\bar{\delta}^\pm = \int_0^1 \bar{\delta}^\pm(\xi) d\xi, \quad (25)$$

and the voltage and current sources ( $V_s$  and  $I_s$ ) are per unit length quantities.

### 3.2 Equivalent Excitation

As with the single coaxial cable, it is desired to develop an equivalent representation that readily lends itself to circuit analysis and point source simulation. The Thevenin equivalent network for the multiconductor cable is a straightforward extension of the coaxial cable development. The source at each end must be an  $n$ -dimensional vector to satisfy the most general conditions. The  $2n$  port impedance matrix now requires  $2n \times 2n$  terms to account for the self and transfer impedances of all the ports. The correctness of the multiconductor Thevenin equivalent network will be examined first. Then the impact of a restriction on the Thevenin source terms will be investigated. The purpose of the source restriction is to further simplify the model.

The response of the shielded multiconductor cable to the Thevenin equivalent source excitation may be obtained from equations (21) through (25). The layout of the Thevenin equivalent network is given in figure 10, where  $V_s^1(0)$  and  $V_s^2(1)$  are the wire to reference open-circuit voltage vectors at  $x = 0$ ,  $x = 1$ , due to the distributed EMP excitation:

$$\begin{bmatrix} \bar{\delta}_d^- \\ \bar{\delta}_d^+ \end{bmatrix} = \frac{1}{2} \int_0^1 \begin{bmatrix} \bar{T} e^{-\gamma \xi} \bar{T}^{-1} \\ \bar{T} e^{\gamma \xi} \bar{T}^{-1} \end{bmatrix} : \begin{bmatrix} \bar{Z}_c^{-1} & \bar{U} \\ \bar{Z}_c^{-1} & -\bar{U} \end{bmatrix} : \begin{bmatrix} \bar{V}_s \\ \bar{I}_s \end{bmatrix}. \quad (26)$$

#### 3.2.1 Thevenin Source Terms

The open circuit voltages  $V^{OC}(0)$  and  $V^{OC}(1)$  are found from equations (21) through (23) and equation (26) if we let the terminating impedances between each wire and the reference conductor, as well as the wire-to-wire impedances, approach infinity (open circuit). The impedance matrix  $Z_1$  may be found from the definition

$$Z_{ij} = V_i/I_j, I_k = 0 \forall k \neq j, \quad (27)$$

yielding

$$Z_{ij} = \begin{cases} \infty, & i=j \\ 0, & i \neq j \end{cases} \quad (28)$$

The source vector  $[\bar{\delta}^-, \bar{\delta}^+]^T$  in equation (26) is independent of the terminating matrices.

The elements of equations (21) through (23) that depend on the termination matrices are of the form

$$\bar{Z}_i [\bar{U} - \bar{\Gamma}_i] = 2\bar{Z}_i [\bar{Z}_i + \bar{Z}_c]^{-1} \bar{Z}_c \quad (29)$$

and

$$\bar{\Gamma}_i = [\bar{Z}_i + \bar{Z}_c]^{-1} [\bar{Z}_i - \bar{Z}_c] \quad (30)$$

In the limit ( $\bar{Z}_i$  defined by eq (28)), it is found that equation (29) approaches  $2\bar{Z}_c$ . The reflection matrix,  $\bar{\Gamma}_i$ , approaches the unit matrix,  $\bar{U}$ , under open circuit conditions.

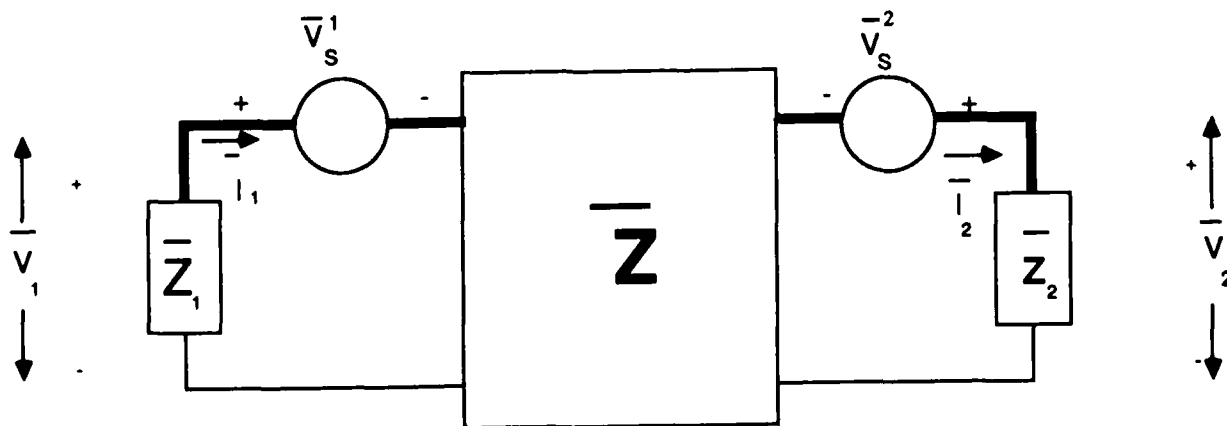


Figure 10. Equivalent source representation for multiconductor transmission line.

Using equations (21) and (22) to define the terminal voltages and taking the limit as the terminating impedances approach infinity yields the following open circuit voltages at the terminals:

$$\begin{bmatrix} \bar{V}^{\text{oc}}(0) \\ \bar{V}^{\text{oc}}(l) \end{bmatrix} = \begin{bmatrix} -2\bar{z}_c & \bar{o} \\ \bar{o} & 2\bar{z}_c \end{bmatrix} : \begin{bmatrix} \bar{U} & \bar{T}e^{-\bar{\gamma}} \bar{T}^{-1} \\ \bar{T}e^{-\bar{\gamma}} \bar{T}^{-1} & \bar{U} \end{bmatrix}^{-1} : \begin{bmatrix} \bar{\delta}_d^- \\ \bar{\delta}_d^+ \end{bmatrix}, \quad (31)$$

with the source terms  $\bar{\delta}_d^-$  and  $\bar{\delta}_d^+$  as given in equation (26).

### 3.2.2 Terminal Response

The terminal response for the Thevenin equivalent network is found by superposition of the response from the source at each end of the cable. The source voltages given in equation (31) are used in conjunction with equation (24) to define the source terms  $\bar{\delta}_p^-$  and  $\bar{\delta}_p^+$  for the current responses given in equation (22). The current source,  $I_s$ , in equation (24) is zero because only a voltage source vector is used at each end of the cable. Summing the source terms due to the voltage sources at  $x_s = 0, l$  yields

$$\begin{aligned} \begin{bmatrix} \bar{\delta}_p^- \\ \bar{\delta}_p^+ \end{bmatrix} &= 1/2 \begin{bmatrix} \bar{z}^{-1} & \bar{T}e^{-\bar{\gamma}} \bar{T}^{-1} \bar{z}_c^{-1} \\ -\bar{T}e^{-\bar{\gamma}} \bar{T}^{-1} \bar{z}_c^{-1} & \bar{z}_c^{-1} \end{bmatrix} : \begin{bmatrix} \bar{V}^{\text{oc}}(0) \\ \bar{V}^{\text{oc}}(l) \end{bmatrix} = \\ &= \begin{bmatrix} \bar{U} & \bar{T}e^{-\bar{\gamma}} \bar{T}^{-1} \\ \bar{T}e^{-\bar{\gamma}} \bar{T}^{-1} & \bar{U} \end{bmatrix} : \begin{bmatrix} \bar{U} & \bar{T}e^{-\bar{\gamma}} \bar{T}^{-1} \\ \bar{T}e^{-\bar{\gamma}} \bar{T}^{-1} & \bar{U} \end{bmatrix}^{-1} : \begin{bmatrix} \bar{\delta}_d^- \\ \bar{\delta}_d^+ \end{bmatrix} \\ &= \begin{bmatrix} \bar{\delta}_d^- \\ \bar{\delta}_d^+ \end{bmatrix}, \end{aligned} \quad (32)$$

where  $\begin{bmatrix} \bar{\delta}_d^- \\ \bar{\delta}_d^+ \end{bmatrix}^T$  is the distributed source term vector. This shows that the Thevenin equivalent network provides the same excitation at the terminals as the distributed excitation. The terminal response is given by equations (21) and (22).

### 3.2.3 Nonlinear Terminations

The nonlinear termination study for a single coaxial line (sect. 2.2.3) is directly applicable to multiconductor lines. The only real question was whether or not Thevenin equivalent circuits of transmission lines are valid with nonlinear terminations. A multiconductor cable simply requires a more complex source and impedance representation. Therefore, the work of section 2.2.3 implies that equivalent circuit representations are valid for multiconductor transmission lines with nonlinear terminations.

### 3.2.4 Coupling Distribution

In the previous sections it was shown that an equivalent source network of  $2N$  independent voltage terms will provide the same terminal response as the distributed excitation. The distribution of the shield coupling parameters among the  $N$  conductors will now be examined in an attempt to further reduce the source requirements.

The distribution of the coupling through the shield will determine the source terms  $V_s$  and  $I_s$  in equation (22). Unfortunately, little work exists on the nature of the coupling distributions. As pointed out in reference [8], most shield coupling studies, both experimental and theoretical, consider coaxially shielded cables with only one conductor. Frankel [8] suggests measurement techniques, but does not provide any insight into the distribution.

In Tigner et al [9], a theoretical treatment is proposed for the distributions of the capacitive and inductive coupling parameters; the common mode inductive and capacitive sources are distributed over the conductors using coupling ratio vectors  $c$  and  $l$  such that

$$\sum_{i=1}^N C_i = 1, \quad \sum_{i=1}^N l_i = 1. \quad (33)$$

The requirement of equation (33) appears plausible for the capacitive coupling parameter since in effect the measured common mode current source is really a set of  $N$  current sources in parallel, each driving one of the wires. However, the requirement that the  $N$  multiconductor voltage sources add up to the common mode voltage sources appears to be inconsistent since the  $N$  voltage sources are also in parallel, not in series as equation (33) suggests. This appears on average to divide the voltage source amplitude by the number of conductors. Evidence of this improper scaling is seen in the results presented by Paul [10] for a comparison of the theoretical model with experimental data. A very large shield transfer impedance of 1 ohm/meter was derived empirically for a 37-conductor cable with a tape-wrapped shield. It is felt that this large shield transfer impedance is an artifact of the requirement of equation (33).

Unfortunately, no other models or experimental data have been discovered in the literature. The following model development attempts to overcome the difficulties discussed above. Only the inductive source is considered in this study. Experimental data suggest that this is the dominant mode of coupling for most good quality shields. Figure 11 presents a section of multiconductor line with an overall shield. The transfer impedance of the shield is  $Z_{ab}$  and the external shield current is  $I_s$  such that the potential along the inside of the shield is

$$V_s = Z_{ab} I_s \Delta x . \quad (34)$$

It is assumed that the external current,  $I_s$ , is evenly distributed around the cable. The line integral of the electric field is related to the surface integral of the magnetic field by Stokes theorem:

$$\int E \cdot dl = -j\omega \int_{\Delta A} B \cdot dA , \quad (35)$$

where  $A$  is the area enclosed by the line integral. Assuming that the distances,  $\Delta x$ , and the wire-to-shield separation are small, the line integral of the electric field may be replaced by the potentials shown in figure 11:

$$V_i(x) - V_i(x + \Delta x) + V_s = -j\omega \int_{\Delta A} B \cdot dA , \quad (36)$$

where the field along the conductor is zero due to the assumption of perfectly conducting wires. Substituting equation (34) for  $V_s$ , dividing by  $x$ , and taking the limit as  $x$  approaches zero yields

$$-\frac{dV(x)}{dx} = -j\omega \int_0^h B \cdot dl - Z_{ab} I_s , \quad (37)$$

with  $h$  being the separation distance of the wire from the shield. The magnetic field,  $B$ , is the total field, incident and scattered. The scattered magnetic field may be related to the wire currents through self and mutual inductances. The incident magnetic field is the field present if the internal wires are not present. However, for frequencies of interest ( $\geq 100$  MHz) and typical cable dimensions (radius  $< 2$  cm) the cable without wires acts as a waveguide well below the cutoff frequency. Therefore, the incident magnetic field is zero, yielding the result that the voltage source on each wire is identical and equal to the product of the transfer impedance and the external current. This does not mean that the open circuit voltages at the ends of the cable are equal, simply that the per unit excitations are equal.

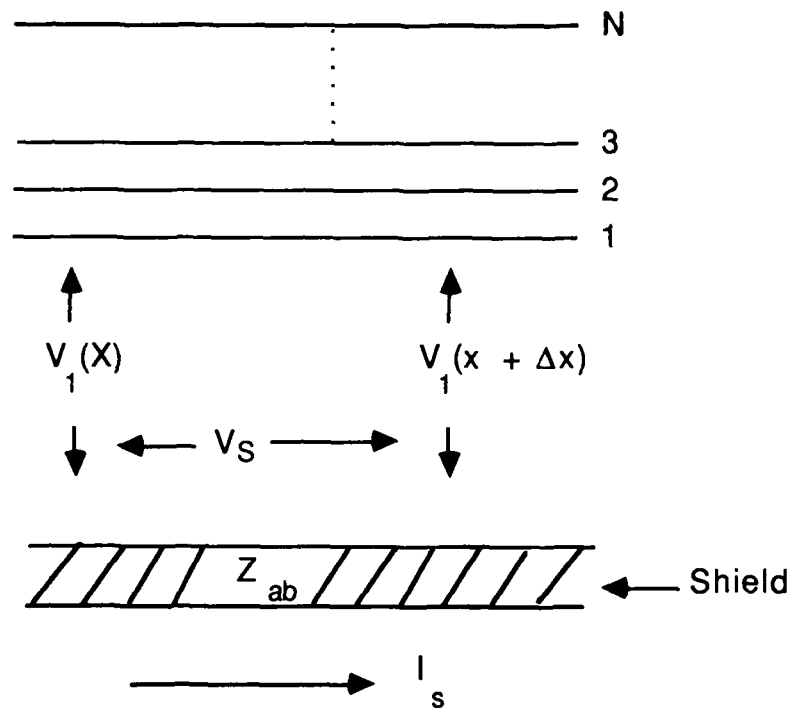


Figure 11. Multiconductor transmission-line segment.

Some insight may be obtained into the open circuit voltage response if a slightly different solution representation is used instead of equations (21), (22), and (24). The chain matrix formulation provided by Paul [10] is as follows:

$$\begin{bmatrix} \bar{V}(l) \\ \bar{I}(l) \end{bmatrix} = \bar{\Phi}(l) \begin{bmatrix} \bar{V}(0) \\ \bar{I}(0) \end{bmatrix} + \int_0^l \bar{\Phi}(l - \hat{\xi}) \begin{bmatrix} \bar{V}_s(\xi) \\ \bar{I}_s(\xi) \end{bmatrix} d\hat{\xi} = \bar{\Phi}(l) \begin{bmatrix} \bar{V}(0) \\ \bar{I}(0) \end{bmatrix} + \begin{bmatrix} \hat{V}_s(l) \\ \hat{I}_s(l) \end{bmatrix}, \quad (38)$$

where

$$\begin{aligned} \hat{V}_s(l) &= \int_0^l \left\{ \bar{\Phi}_{11}(l - \xi) \bar{V}_s(\xi) + \bar{\Phi}_{12}(l - \xi) \bar{I}_s(\xi) \right\} d\xi \\ \hat{I}_s(l) &= \int_0^l \left\{ \bar{\Phi}_{21}(l - \xi) \bar{V}_s(\xi) + \bar{\Phi}_{22}(l - \xi) \bar{I}_s(\xi) \right\} d\xi \end{aligned} \quad (39)$$

and

$$\begin{aligned}
\bar{\Phi}_{11}(l) &= \bar{C}^{-1} \bar{T} \cosh(j\omega\bar{\gamma}l) \bar{T}^{-1} \bar{C} & \bar{\Phi}_{21}(l) &= -\bar{T} \sinh(j\omega\bar{\gamma}l) \bar{T}^{-1} \bar{Z}_c^{-1} \\
\bar{\Phi}_{12}(l) &= -\bar{Z}_c \bar{T} \sinh(j\omega\bar{\gamma}l) \bar{T}^{-1} & \bar{\Phi}_{22}(l) &= \bar{T} \cosh(j\omega\bar{\gamma}l) \bar{T}^{-1}.
\end{aligned} \tag{40}$$

The open circuit voltage may be found from equations (36) through (38) if we simply let  $I(0)$  and  $I(l)$  equal zero.

Now consider the simple condition where the current source  $I_s$  is negligible, and also assume that the external shield current is constant over the length of the cable. Then the open circuit voltage at the  $x = 0$  end becomes

$$\begin{aligned}
\bar{V}(0) &= \left[ \bar{\Phi}_{21}^{-1}(l) \int_0^l \bar{\Phi}_{21}(l-\xi) d\xi \right] \bar{V}_s \\
&= \left[ \bar{Z}_c \bar{T} \left[ \sinh j\omega\bar{\gamma}l \right]^{-1} \int_0^l \sinh j\omega\bar{\gamma}(l-\xi) \bar{T}^{-1} \bar{Z}_c^{-1} d\xi \right] \bar{V}_s \\
&= \bar{Z}_c \bar{T} \left[ j\omega\bar{\gamma} \sinh j\omega\bar{\gamma}l \right]^{-1} \left[ \cosh j\omega\bar{\gamma}l - 1 \right] \bar{T}^{-1} \bar{Z}_c^{-1} \bar{V}_s.
\end{aligned} \tag{41}$$

The open circuit voltage at the other end is identical except for the sign. If the dielectric is homogeneous then the transformation matrix  $\bar{T}$  is the unit matrix and the eigenvalue matrix,  $\bar{\gamma}$ , becomes

$$\bar{\gamma} = \frac{1}{v} \bar{U}, \tag{42}$$

where  $v$  is the propagation velocity of the line. Then the open circuit voltage becomes

$$\bar{V}(0) = \frac{v \left( \cosh \frac{j\omega l}{v} - 1 \right)}{j\omega \sinh j \frac{\omega l}{v}} \bar{V}_s, \tag{43}$$

which means that the open circuit voltage is constant for all the wires if the source voltage,  $\bar{V}_s$ , is constant. The open circuit voltage at  $x = l$  is identical except for the sign. A similar result may be obtained for the current-source-only condition, except the sign does not change from end to end.

If the cable is not homogeneous then there may be distinct eigenvalues. Since the eigenvalue matrix  $\tilde{Y}$  is diagonal, equation (41) may be rewritten as

$$V(o) = \bar{Z}_c \bar{T} \begin{bmatrix} v_1 \left( \cosh \frac{j\omega l}{v_1} - 1 \right) \\ \frac{j\omega \sinh j \frac{\omega l}{v_1}}{v_1} \\ \vdots \\ 0 \\ \vdots \\ v_N \left( \cosh \frac{j\omega l}{v_N} - 1 \right) \\ \frac{j\omega \sinh \frac{j\omega l}{v_N}}{v_N} \\ 0 \end{bmatrix} \bar{T}^{-1} \bar{Z}_c^{-1} \bar{V}_s, \quad (44)$$

and the open circuit voltage vector will not be constant even if  $V_s$  is constant. The amplitude of each mode is proportional to its propagation velocity,  $v_i$ , and the wire potentials are weighted sums of these mode voltages with the weights determined by the T matrix and the characteristic impedance matrix,  $\bar{Z}_c$ .

Therefore, under the assumptions of inductive coupling dominance and a homogeneous dielectric the open circuit voltage from each wire to the shield will be equal. This means that a single source may be used in series with the cable shield at each end of the cable. This allows a significant reduction in the complexity of a Thevenin equivalent network for multiconductor cables. Now only two sources are needed, not  $2N$ . For nonhomogeneous dielectrics, the variation in wire to shield potentials may be small enough to allow use of only one source at each end. The suitability of this approximation will depend on the specific characteristics of the cable under study. Implementation details are discussed in the following section.

### 3.3 Equivalent Excitation Implementation

There are at least three implementation techniques that can be used in the simulation of the EMP response of a shielded cable. The purpose of discussing implementation techniques here is to provide theoretical insight into each method and to discuss the advantages and disadvantages of each. The discussion is limited to implementation on physical systems since circuit analysis modeling is relatively straightforward.

If it is known that the open circuit voltages are widely different for each of the  $N$  conductors, then the only implementation possible is the development of independent sources for each of the  $2N$  ports. These sources must be reasonable approximations to ideal voltage sources. This requires the

source impedances to be much smaller than the characteristic impedances of the cable. The sources are placed in series with each conductor.

Of most interest here is the condition discussed in section 2.2.4, where the open circuit voltages are all approximately equal at each end of the cable. Then only two sources are needed, one for each end. These sources must be inserted into the reference conductor (the cable shield). The simplest way to implement these sources is to insert very low resistance in series with the cable shield and create the required voltage waveform across these resistors; see figure 12. The sources must provide currents defined by

$$I_s(x) = V_{oc}(x)/R, x = 0, 1, \quad (45)$$

where the resistance,  $R$ , must be much less than the bundle-to-shield impedance of the cable. The key advantages of this method are low power requirements and ease of specifying the source waveforms. The major disadvantage is that the shield continuity is disrupted by the insertion of the resistors.

A tradeoff may be made between the advantages and disadvantages of the simple resistive insertion technique. The integrity of the shield may be preserved if a segment of the shield is used instead of resistors to obtain the low source impedance. The source current waveform is then defined by

$$I_s(x) = V_{oc}(x)/(R_s + j\omega L_s)dx, x = 0, 1, \quad (46)$$

where  $R_s$  and  $L_s$  are the per unit length shield resistance and inductance, and  $dx$  is the length of the source segment. Equation (46) assumes that the shield excitation is dominated by the resistive-inductive transfer impedance and that the segment length,  $dx$ , is short compared to the smallest wavelength of the open circuit voltage. The preservation of the shield is obtained at the expense of the source current requirement. Typical shield transfer impedances range from 1 to 10 milliohms per meter, whereas the source resistance,  $R$ , may be as large as 1 ohm in some instances and still satisfy the requirement of being much less than the bundle-to-shield impedance. Therefore, the source current requirements may go up as much as an order of magnitude or more. The sources can be connected to the shield segments if some of the insulation at the ends of the cable is removed or if a short extension is added to the cable. The main advantage of this method is the preservation of the external shield integrity. The primary disadvantage is the high source current required, with a secondary problem being the difficulty associated with the physical connection to the shield.

The third technique attempts to reduce the disadvantages of the second technique through excitation of the entire cable shield as shown in figure 13. This technique has a much more complicated source specification because of the very distributed nature of the coupling through the shield. The source current is given in the frequency domain by

$$I_s(x) = V_{oc}(x)/V_d(x), x = 0, 1 \quad (47)$$

where  $V_d(x)$  is defined as the open circuit bundle voltage due to an impulse function excitation (constant frequency spectrum). An analytical expression for  $V_d(x)$  may be obtained from equation (4), with the voltage and current sources being functions of the external response to the impulse functions. This analysis is similar in complexity to the normal EMP analysis of the cable. It is also possible to determine  $V_d(x)$  experimentally. The advantages offered by this technique are a slightly better source power requirement over the shield segment technique and complete maintenance of the shield integrity. The disadvantages are (1) a more complex source specification and (2) the possibility that the source current may not be a realizable function due to nulls or peaks in  $V_d(x)$ .

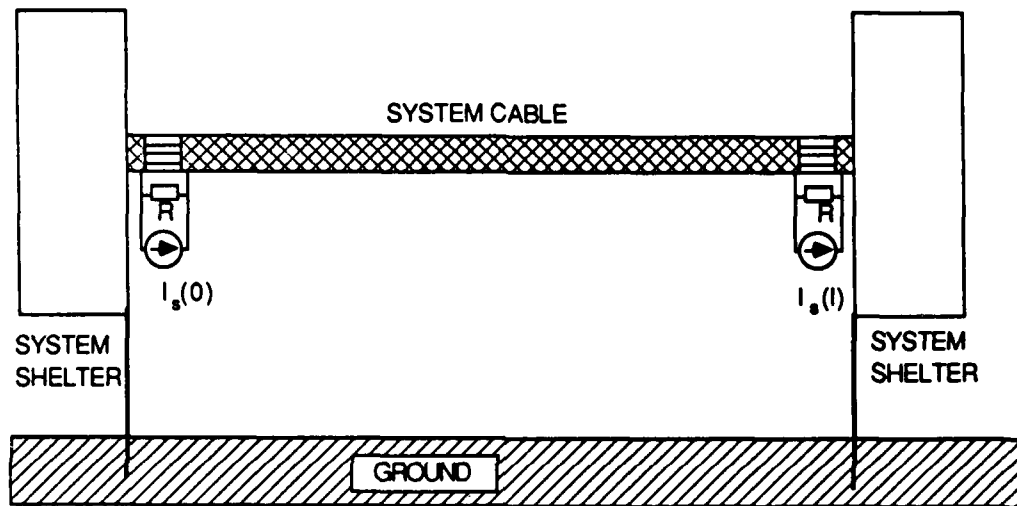


Figure 12. Equivalent source implementation using resistors in shield.

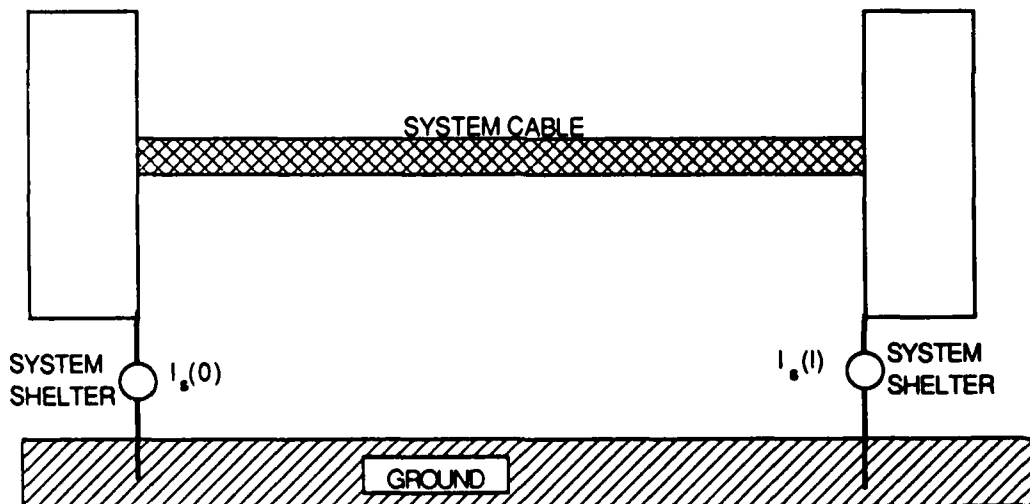


Figure 13. Equivalent source implementation over entire cable shield.

#### 4. CONCLUSION

Efficient equivalent source representations were developed for coaxially shielded cables and for multiconductor cables. The correctness of these equivalent source representations was validated for linear and nonlinear terminations. The distribution of shield coupling parameters was studied for shielded multiconductor cables. The results of this study indicate that an approximate equivalent source excitation may be used for multiconductor cables, thereby reducing the source requirements even further. The approximate equivalent source excitation requires only two independent sources to represent the EMP response of the cable. The simplicity of the equivalent source excitation means that numerical models will run quicker, and system-level stimulation is possible with a lower power level and less complex simulators.

#### REFERENCES

1. K. F. Casey and E. F. Vance, EMP Coupling Through Cable Shields, IEEE Trans. Antennas Propag. AP-26 (January 1978), 100-106.
2. Dikewood Industries, Inc., EMP Interaction: Principles, Techniques and Reference Data (A Complete Concatenation of Technology from the EMP Interaction Notes), EMP Interaction 2-1 (December 1980).
3. R. F. Gray and N. V. Hill, EMP Coupling to Coaxially Shielded Cables: Computer Program FREFLD Development and Use, Harry Diamond Laboratories, HDL-TR-2076 (December 1986).
4. S. A. Schelkunoff, The Electromagnetic Theory of Coaxial Transmission Lines and Cylindrical Shields, Bell Syst. Tech. J., 13 (October 1934).
5. E. P. Peskin, Transient and Steady-State Analysis of Electric Networks, Boston Technical Publishers (1965).
6. R. F. Gray, Note 1: Analysis of a Simple Transmission Line with Nonlinear Loading, Synchronous Injection Techniques Note Series, ENSCO, Inc., (April 1986).
7. F. M. Teshe, T. K. Liu, S. K. Chang, and D.V. Giri, Air Force Weapons Laboratory, AFWL Interaction Notes, Note 351 (September 1978).
8. S. Frankel, Terminal Response of Braided-Shield Cables to External Monochromatic Electromagnetic Fields, Harry Diamond Laboratories, HDL-TR-1602 (August 1972).
9. J. E. Tigner, M. J. Schmidt, P. N. Setty, and S. T. Ives, The Excitation of Multiconductor Bundles of Wires by Electric and Magnetic Cavity Fields, IEEE Transactions on Nuclear Science, NS-27, 6 (December 1980).
10. C. R. Paul, Efficient Numerical Computation of the Frequency Response of Cables Illuminated by an Electromagnetic Field, IEEE Transactions on Microwave Theory and Techniques (April 1974).

DISTRIBUTION

ADMINISTRATOR  
DEFENSE TECHNICAL INFORMATION CENTER  
CAMERON STATION, BUILDING 5  
ATTN DTIC-DDA (12 COPIES)  
ALEXANDRIA, VA 22304-6145

ASSISTANT TO THE SECRETARY OF DEFENSE  
ATOMIC ENERGY  
ATTN EXECUTIVE ASSISTANT  
WASHINGTON, DC 20301

DIRECTOR  
DEFENSE COMMUNICATIONS AGENCY  
ATTN CODE B410  
ATTN CODE B430  
WASHINGTON, DC 20305

DIRECTOR  
COMMAND CONTROL ENGINEERING CENTER  
ATTN C-660  
ATTN G-630  
WASHINGTON, DC 20305

DIRECTOR  
DEFENSE COMMUNICATIONS ENGINEERING CENTER  
ATTN CODE R400  
ATTN CODE R123, TECH LIB  
ATTN CODE R111  
1860 WIEHLE AVENUE  
RESTON, VA 22090

ASSISTANT CHIEF OF STAFF FOR  
INFORMATION MANAGEMENT  
COMMAND SYSTEMS INTEGRATION OFFICE  
ATTN DAMO-C4Z  
THE PENTAGON  
WASHINGTON, DC 20301

DIRECTOR  
DEFENSE INTELLIGENCE AGENCY  
ATTN DB-4C2, D. SPOHN  
WASHINGTON, DC 20301

CHAIRMAN  
JOINT CHIEFS OF STAFF  
ATTN J-3  
ATTN C3S  
WASHINGTON, DC 20301

NATIONAL COMMUNICATIONS SYSTEM  
DEPARTMENT OF DEFENSE  
OFFICE OF THE MANAGER  
ATTN NCS-TS, D. BODSON  
WASHINGTON, DC 20305

DIRECTOR  
DEFENSE NUCLEAR AGENCY  
ATTN RAEV  
ATTN DDST  
ATTN RAEF

DIRECTOR  
DEFENSE NUCLEAR AGENCY (cont'd)  
ATTN TITL  
WASHINGTON, DC 20305

OFFICE OF UNDERSECRETARY OF DEFENSE  
RESEARCH & ENGINEERING  
DMSSO  
2 SKYLINE PLACE  
SUITE 1403  
5203 LEESBURG PIKE  
FALLS CHURCH, VA 22041

UNDER SECY OF DEF FOR RSCH & ENGRG  
DEPARTMENT OF DEFENSE  
ATTN STRATEGIC & SPACE SYS 90SO RM 3E129  
ATTN STRAT & THEATER NUC FORCES  
WASHINGTON, DC 20301

DEPUTY DIRECTOR FOR THEATRE/TACTICAL C3  
SYSTEMS  
JOINT STAFF  
WASHINGTON, DC 20301

COMMANDER-IN-CHIEF  
US FORCES, EUROPE  
ATTN ECC3S  
APO, NY 09128

ASSISTANT CHIEF OF STAFF FOR  
AUTOMATION & COMMUNICATIONS  
ATTN DAMO-C4T  
ATTN DAMO-C4S  
DEPARTMENT OF THE ARMY  
WASHINGTON, DC 20360

US ARMY BALLISTIC RESEARCH  
LABORATORY  
ATTN DRDAR-TSB-S (STINFO)  
ABERDEEN PROVING GROUND, MD 21005

COMMANDER  
US ARMY INFORMATION SYSTEMS COMMAND  
ATTN CC-OPS-WR, O.P. CONNELL/R. NELSON  
FT HUACHUCA, AZ 85613

US ARMY COMBAT SURVEILLANCE & TARGET  
ACQUISITION LABORATORY  
ATTN DELET-DD  
FT MONMOUTH, NJ 07703

COMMANDER  
US ARMY ELECTRONIC SYSTEMS ENGINEERING  
INSTALLATION AGENCY  
ATTN ASBH-SET-S  
FORT HUACHUCA, AZ 85613

DISTRIBUTION (cont'd)

US ARMY ENGINEER DIV HUNTSVILLE  
DIVISION ENGINEER  
ATTN HNDED FD,  
PO BOX 1600  
HUNTSVILLE, AL 35807

COMMANDER  
US ARMY INFORMATION SYSTEMS  
ENGINEERING COMMAND  
SUPPORT ACTIVITY  
ATTN ASB-TS-A, B. EGBERT  
FORT MONMOUTH, NJ 07703-5000

COMMAND  
US ARMY MATERIEL COMMAND  
ATTN DRCRE  
ATTN DRCDE  
5001 EISENHOWER AVE  
ALEXANDRIA, VA 22333-0001

DIRECTOR  
US ARMY MATERIEL SYSTEMS ANALYSIS  
ACTIVITY  
ATTN DRXSY-MP, LIBRARY  
ABERDEEN PROVING GROUND, MD 21005

COMMANDER  
US ARMY MISSILE COMMAND  
ATTN DRCPM-CF, CHAPARRAL/FAAR  
ATTN DRCPM-HD, HELLFIRE/GLD  
ATTN DRCPM-PE, PERSHING  
ATTN DRCPM-DT, TOW DRAGON  
ATTN DRCPM-RS, GENERAL SUPPORT  
ROCKET SYS  
ATTN DRCPM-HEL, HIGH ENERGY LASER SYS  
ATTN DRCPM-ROL, ROLAND  
ATTN DRCPM-VI, VIPER  
ATTN DRCPM-HA, HAWK  
ATTN DRCPM-MP, STINGER  
ATTN DRSMI-T, TARGETS MANAGEMENT OFFICE  
ATTN DRSMI-U, WEAPONS SYS MGT DIR  
ATTN DRSMI-D, PLANS, ANALYSIS,  
& EVALUATION  
ATTN DRSMI-E, ENGINEERING  
ATTN DRSMI-Q, PRODUCT ASSURANCE  
ATTN DRSMI-S, MATERIEL MANAGEMENT  
ATTN DRSMI-W, MGMT INFO SYSTEMS  
REDSTONE ARSENAL, AL 35809

DIRECTOR  
US ARMY MISSILE LABORATORY  
USAMICOM  
ATTN DRSMI-RPR, REDSTONE SCIENTIFIC  
INFO CENTER  
ATTN DRSMI-RPT, TECHNICAL  
INFORMATION DIV  
ATTN DRSMI-RN, CHIEF, TECHNOLOGY  
INTEGRATION OFFICE  
ATTN DRSMI-RA, CHIEF, DARPA PROJECTS  
OFFICE

DIRECTOR  
US ARMY MISSILE LABORATORY  
USAMICOM (cont'd)  
ATTN DRSMI-RH, DIR, DIRECTED ENERGY  
DIRECTORATE  
ATTN DRSMI-RL, SPE ASST GROUND EQUIP &  
MISSILE STRUCTURES DIR  
ATTN DRSMI-RR, RESEARCH DIR  
ATTN DRSMI-RS, SYS ENGR DIR  
ATTN DRSMI-RT, TEST & EVAL DIR  
ATTN DRSMI-RD, SYST SIMULATION & DEV DIR  
ATTN DRSMI-RE, ADVANCED SENSORS DIR  
ATTN DRSMI-RK, PROPULSION DIR  
ATTN DRSMI-RG, GUIDANCE & CONTROL DIR  
REDSTONE ARSENAL, AL 35809

COMMANDER  
US ARMY MISSILE & MUNITIONS  
CENTER & SCHOOL  
ATTN ATSK-CTD-F  
REDSTONE ARSENAL, AL 35809

COMMANDER  
US ARMY NUCLEAR & CHEMICAL AGENCY  
ATTN MONA-WE  
7500 BACKLICK ROAD  
SPRINGFIELD, VA 22150

DEP CH OF STAFF FOR RSCH, DEV, & ACQ  
DEPARTMENT OF THE ARMY  
ATTN DAMA-CSS-N  
WASHINGTON, DC 20310

CHIEF  
US ARMY SATELLITE COMMUNICATIONS  
AGENCY  
ATTN DRCPM-SC  
FT MONMOUTH, NJ 07703

DIRECTOR  
TRI/TAC  
ATTN TT-E-SS, CHARNICK  
FT MONMOUTH, NJ 07703

COMMANDANT  
US ARMY WAR COLLEGE  
ATTN LIBRARY  
CARLISLE BARRACKS, PA 17013

COMMANDER-IN-CHIEF  
ATLANTIC  
ATTN J6  
NORFOLK, VA 23511

COMMANDER  
NAVAL ELECTRONIC SYSTEMS COMMAND  
ATTN PME 110-241D  
WASHINGTON, DC 20360

DISTRIBUTION (cont'd)

NAVAL ELECTRONICS ENGINEERING ACTIVITY,  
PACIFIC  
BOX 130  
ATTN DON O'BRYHIM  
PEARL HARBOR, HAWAII 96860-5170

CHIEF OF NAVAL MATERIEL  
THEATER NUCLEAR WARFARE PROJECT OFFICE  
ATTN PM-23  
WASHINGTON, DC 20360

COMMANDER  
NAVAL OCEAN SYSTEMS CENTER  
ATTN CODE 83, J. STAWISKI  
SAN DIEGO, CA 92152

COMMANDING OFFICER  
NAVAL ORDNANCE STATION  
ATTN STANDARDIZATION DIVISION  
INDIAN HEAD, MD 20640

COMMANDER-IN-CHIEF  
PACIFIC  
ATTN C3S-RP-1  
CAMP H. M. SMITH, HI 96861

COMMANDING OFFICER  
NAVAL RESEARCH LABORATORY  
ATTN CODE 4720, J. DAVIS  
WASHINGTON, DC 20375

COMMANDER  
NAVAL SURFACE WEAPONS CENTER  
ATTN CODE F-56  
DAHLGREN, VA 22448

COMMANDER  
NAVAL SURFACE WEAPONS CENTER  
ATTN CODE F32, E. RATHBURN  
ATTN CODE F30  
WHITE OAK LABORATORY  
SILVER SPRING, MD 20910

DEPARTMENT OF THE NAVY  
DIRECTOR, NAVAL TELECOMMUNICATIONS  
DIVISION  
OFFICE OF THE CHIEF OF NAVAL OPERATIONS  
ATTN OP941, HAISLMAIER  
ATTN OP943  
WASHINGTON, DC 20350

HQ, USAF/SAMI  
WASHINGTON, DC 20330

AIR FORCE COMMUNICATIONS COMMAND  
ATTN EPPD  
SCOTT AFB, IL 62225

COMMANDER  
US AIR FORCE SPACE COMMAND  
ATTN KRQ  
ATTN XPOW  
PETERSON AFB, CO 80912

1842 EEG  
ATTN EEISG  
SCOTT AFB, IL 62225

HEADQUARTERS  
ELECTRONIC SYSTEMS DIVISION/YS  
ATTN YSEA  
HANSCOM AFB, MA 01730

HEADQUARTERS  
USAFE  
ATTN DCKI  
RAMSTEIN AFB, GERMANY

SYSTEM INTEGRATION OFFICE  
ATTN SYE  
PETERSON AFB, CO 80912

AIR FORCE WEAPONS LABORATORY/DYC  
ATTN NTC4, TESD, IESM  
KIRTLAND AFB, NM 87117

CENTRAL INTELLIGENCE AGENCY  
ATTN OWSR/NED  
WASHINGTON, DC 20505

DIRECTOR  
FEDERAL EMERGENCY MANAGEMENT AGENCY  
NATIONAL PREPAREDNESS PROGRAM SUPPORT  
ATTN OFFICE OF RESEARCH  
WASHINGTON, DC 20472

DIRECTOR  
FEDERAL EMERGENCY MANAGEMENT AGENCY  
STATE & LOCAL SUPPORT BR  
ATTN SL/EM/SS/LS, LOGISTICS  
SUPPORT BRANCH  
WASHINGTON, DC 20472

LAWRENCE LIVERMORE NATIONAL LAB  
ATTN TECHNICAL INFO DEPT LIBRARY  
ATTN L-156, H. CABAYAN, L. MARTIN  
PO BOX 808  
LIVERMORE, CA 94550

DIRECTOR  
NATIONAL SECURITY AGENCY  
ATTN R15  
9800 SAVAGE ROAD  
FT MEADE, MD 20755

DISTRIBUTION (cont'd)

AMERICAN TELEPHONE & TELEGRAPH CO  
ATTN SEC OFC FOR W. EDWARDS  
1120 20TH STREET, NW  
WASHINGTON, DC 20036

AT&T BELL LABORATORIES  
ATTN R. STEVENSON  
ATTN J. MAY  
1600 OSGOOD ST  
N. ANDOVER, MA 01845

AT&T BELL LABORATORIES  
ATTN J. SERRI  
CRAWFORDS CORNER ROAD  
HOLMDEL, NJ 07733

BDM CORP  
ATTN CORPORATE LIBRARY  
7915 JONES BRANCH DRIVE  
McLEAN, VA 22102

BOEING CO  
PO BOX 3707  
ATTN R. SHEPPE  
SEATTLE, WA 98124

ENERGISTICS CORP  
ATTN R. MANRIQUEZ  
1125 JEFFERSON DAVIS HWY  
SUITE 1500  
ARLINGTON, VA 22202

ENGINEERING SOCIETIES LIBRARY  
ATTN ACQUISITIONS DEPT  
345 E. 47TH ST  
NEW YORK, NY 10017

ENSCO, INC  
ATTN R. GRAY (15 COPIES)  
540 PORT ROYAL RD  
SPRINGFIELD, VA 22151

GEORGIA INSTITUTE OF TECHNOLOGY  
OFFICE OF CONTRACT ADMINISTRATION  
ATTN RES & SEC COORD FOR H. DENNY  
ATLANTA, GA 30332

IIT RESEARCH INSTITUTE  
ATTN J. BRIDGES  
ATTN I. MINDEL  
10 W 35TH STREET  
CHICAGO, IL 60616

INTERNATIONAL TEL & TELEGRAPH CORP  
ATTN A. RICHARDSON  
ATTN TECHNICAL LIBRARY  
500 WASHINGTON AVENUE  
NUTLEY, NJ 07110

MARTIN MARIETTA CORPORATION  
PO BOX 5837  
ATTN DR. C. WHITESCARVER  
ORLANDO, FL 32805

MISSION RESEARCH CORP  
ATTN TOM BOLT  
735 STATE STREET  
SANTA BARBARA, CA 93102

MISSION RESEARCH CORP  
ATTN W. STARKE  
PO BOX 7816  
COLORADO SPRINGS, CO 80933

MISSION RESEARCH CORP  
EM SYSTEM APPLICATIONS DIVISION  
ATTN A. CHODOROW  
1720 RANDOLF ROAD, SE  
ALBUQUERQUE, NM 87106

PRI, INC  
ATTN W. HAAS  
6121 LINCOLNIA RD  
ALEXANDRIA, VA 22312

R&D ASSOCIATES  
ATTN W. GRAHAM  
PO BOX 9695  
MARINA DEL REY, CA 90291

R&D ASSOCIATES  
ATTN DIRECTOR, DR. J. THOMPSON  
1401 WILSON BLVD  
SUITE 500  
ARLINGTON, VA 22209

ROCKWELL INTERNATIONAL CORP  
ATTN D/243-068, 031-CA31  
PO BOX 3105  
ANAHEIM, CA 92803

SCIENCE ENGINEERING ASSOC  
ATTN P. FLEMMING  
ATTN V. JONES  
PO BOX 31819  
701 DEXTER AVE, N  
SEATTLE, WA 98109-4318

SRI INTERNATIONAL  
ATTN A. WHITSON  
ATTN E. VANCE  
333 RAVENSWOOD AVENUE  
MENLO PARK, CA 94025

DISTRIBUTION (cont'd)

TRW DEFENSE & SPACE SYSTEMS GROUP  
ATTN J. PENAR  
ONE SPACE PARK  
REDONDO BEACH, CA 92078

TRW DEFENSE & SPACE SYSTEMS GROUP  
ATTN E. P. CHIVINGTON  
2240 ALAMO, SE  
SUITE 200  
ALBUQUERQUE, NM 87106

US ARMY LABORATORY COMMAND  
ATTN TECHNICAL DIRECTOR, AMSLC-TD  
ATTN PUBLIC AFFAIRS, AMSLC-PA

INSTALLATION SUPPORT ACTIVITY  
ATTN LEGAL OFFICE, SLCIS-CC

USAISC  
ATTN RECORD COPY, ASNC-ADL-TS  
ATTN TECHNICAL REPORTS BRANCH,  
ASNC-ADL-TR (3 COPIES)

HARRY DIAMOND LABORATORIES  
ATTN D/DIVISION DIRECTORS  
ATTN LIBRARY, SLCHD-TL (3 COPIES)  
ATTN LIBRARY, SLCHD-TL (WOODBIDGE)  
ATTN LAB DIRECTOR, SLCHD-NW-E  
ATTN CHIEF, SLCHD-NW-EC  
ATTN CHIEF, SLCHD-NW-ED  
ATTN CHIEF, SLCHD-NW-EE  
ATTN CHIEF, SLCHD-NW-P  
ATTN CHIEF, SLCHD-NW-R  
ATTN CHIEF, SLCHD-NW-RA  
ATTN CHIEF, SLCHD-NW-RC  
ATTN CHIEF, SLCHD-NW-RH  
ATTN CHIEF, SLCHD-NW-RI  
ATTN CHIEF, SLCHD-TT  
ATTN R. GOODMAN, SLCHD-DE-OS  
ATTN B. ZABLUDOWSKI, SLCHD-IT-EB  
ATTN J. O. WEDEL, JR., SLCHD-IT-EB  
ATTN RONALD J. CHASE, SLCHD-NW-EC  
ATTN W. SCOTT, SLCHD-NW-EE  
ATTN J. W. BEILFUSS, SLCHD-NW-ED (15 COPIES)